Heliyon 9 (2023) e22139

Contents lists available at ScienceDirect

Heliyon

journal homepage: www.cell.com/heliyon

Mapping biochemical and nutritional changes in durum wheat due to spoilage during storage

Navnath S. Indore [a], Chithra Karunakaran [a,b], Digvir S. Jayas [a,c,*], Viorica F. Bondici [b], Miranda Vu [b], Kaiyang Tu [b], David Muir [b]

[a] Biosystems Engineering, University of Manitoba, Winnipeg, MB R3T 5V6, Canada
[b] Canadian Light Source Inc., Saskatoon, SK S7N 2V3, Canada
[c] President's Office, A762 University Hall, University of Lethbridge, Lethbridge, AB T1K 3M4 Canada

ARTICLE INFO

Keywords:
Synchrotron
durum wheat
X-ray fluorescence spectroscopy
X-ray fluorescence imaging
Mid-infrared spectroscopy
Post-harvest storage

ABSTRACT

Synchrotron X-ray imaging and spectroscopy techniques were used for studying changes during post-harvest storage of food grains. Three varieties (AAC Spitfire, CDC Defy, and AAC Stronghold) of the Canada Western Amber Durum (CWAD) wheat class were stored for five weeks at 17 % moisture content (wb). Control (dry) and stored moistened seeds were analyzed for biochemical and nutritional changes using synchrotron bulk X-ray fluorescence spectroscopy (SR-XRF), X-ray fluorescence imaging (SR-XFI), and mid-infrared (mid-IR) spectroscopy at the Canadian Light Source (CLS), Saskatoon, SK. All varieties of durum wheat were spoiled at the end of five week, and AAC Spitfire and CDC Defy varieties were most affected in nutritional composition and their distribution than AAC Stronghold. Variable response to changes in biochemical and nutrition were found in all three spoiled varieties of the same durum wheat class.

1. Introduction

Durum wheat is the 10th most important cereal cultivated worldwide [1] with an annual production of average of 40 million tonnes (Mt). Durum wheat is an important cereal crop of Canada because Canada leads the export of durum wheat in the world. The total economic impact on Canadian economy from durum wheat sector was 7.5 billion CAD per year during 2018-20 [2]. Canada produced around 6.11 Mt of durum wheat and exported around 2.71 Mt in 2022 [3]. There is a demand for good quality durum wheat, and Canada shares 50 % of the world's export of durum wheat [4]. Canadian durum wheat is bright yellow in color with high protein content and semolina yield, making it an excellent choice for making high-quality food products. Durum wheat is a cereal crop and cereal food grains face many challenges during bulk storage. Cereal grains are stored at many points along the food chain for a short or long time before consumption, where sound grain storage management plays an important role in keeping post-harvest losses to a minimum. The post-harvest losses in cereals range from 1 % in well managed systems to 50 % in poorly managed systems [5]. Sometimes, in a single unit of storage, total grain can be spoiled, making it unsuitable for human consumption, thus resulting in 100 % loss [5]. The high moisture content leads to the growth of fungi on food grains under favourable temperatures. It is necessary to study changes in the quality of wheat during storage; therefore many studies had been conducted to develop better post-harvest guidelines [4,6–11]. Food grains have unique internal features, structures, and compositions that differentiate them from each other in classes

* Corresponding author. Biosystems Engineering, University of Manitoba, Winnipeg, MB R3T 5V6, Canada.
E-mail address: digvir.jayas@umanitoba.ca (D.S. Jayas).

https://doi.org/10.1016/j.heliyon.2023.e22139
Received 3 July 2023; Received in revised form 21 October 2023; Accepted 5 November 2023
Available online 8 November 2023

and varieties. Therefore, the use of non-destructive methods such as X-ray imaging for the study of changes in storage has taken place in the last two decades. The conventional X-ray imaging system for wheat [12–16] was used to determine various structural features for seed characterisation. The wheat seed crease depth and morphology of two wheat lines were compared to reveal diseases such as black spots that infect particularly at the crease [17]. These conventional systems have certain limitations such as low resolution, more scanning time, and non-selective wavelength. Therefore, synchrotron X-ray imaging techniques have gained pace in the last two decades and are used by researchers across the globe.

Soft wheat cultivars have better post-harvest storage tolerance than harder cultivars [18] and durum wheat is hard wheat, hence it has poor storability than other non-durum wheat [4]. The wheat structure and nutritional composition might play an important role in the resistance to deterioration. However, knowledge about changes in nutrients or study on effect of storage on nutrient presence using advanced imaging is limited. Wheat has micro-nutrients: Mn, Fe, Cu, and Zn; and macro-nutrients: Na, Mg, K and Ca [19]. Micro- and macro-nutrients may play a role in fungal pathogen defense for plants or wheat seeds. The roles of micronutrients in plant defense have been documented for Mn, Fe, Cu, and Zn [20–22]. Synchrotron X-ray fluorescence imaging and spectroscopy are widely used in agricultural and medical sciences and have potential for determining nutritional components in seeds. The changes in nutrient presence and mapping using synchrotron X-ray based fluorescence imaging in wheat crops were reported during crop growth stages, and effect of various fertilizer treatments but not visualized in post harvest storage studies. It has been used in pea seeds [23] for bulk nutritional analysis, whole wheat sections [24], and in cereals [24–27].

Wheat has about 78 % carbohydrates, 14 % protein, 2 % lipids, and 2.5 % minerals [28] and durum wheat is generally characterized by its high amounts of protein (14.3–15.1 %) [29,30]. Fungal infection of wheat seeds can cause significant changes in the biochemical components [31]. The storage protein of wheat has immense importance in determining the quality and end-use properties of the grain, which means it has some role to play during safe storage [32]. Mid-IR spectroscopy was used along with synchrotron imaging techniques for the identification of *Fusarium* resistant wheat variety [33], high nutritional value pea seeds [34], changes in stored wheat due to fungal damage [35], and synchrotron infrared microscopy was also used for analyses of animal feed quality [36]. Therefore, this study was conducted to characterize the durum wheat varieties based on nutritional and biochemical changes in storage due to spoilage. Our study hypothesizes that, spoilage in storage can have an impact on nutritional and biochemical composition of durum wheat, and each variety under the durum wheat class can behave differently. The generated data for durum wheat can be beneficial for making storage decisions and for the food processing industry. Information about the changes in nutrition using advanced imaging, like synchrotron imaging, is limited in post harvest storage studies of cereals; therefore, this work was undertaken to understand the behaviour of nutritional changes due to spoilage in durum wheat during bulk storage. The objectives of this study were to 1) determine nutrient composition using synchrotron X-ray fluorescence spectroscopy (SR-XRF) and localization using synchrotron X-ray fluorescence imaging (SR-XFI) and 2) determine the biochemical composition by mid-infrared (mid-IR) spectroscopy. The developed methodology of this study can be used for assessing changes in other Canadian wheat classes during storage.

2. Materials and methods

2.1. Wheat

In this study, we procured and used commercially available certified seeds of Canada Western Amber Durum wheat (varieties: CDC Defy, AAC Stronghold, and AAC Spitfire) from a company (SeCan, Niverville, MB).

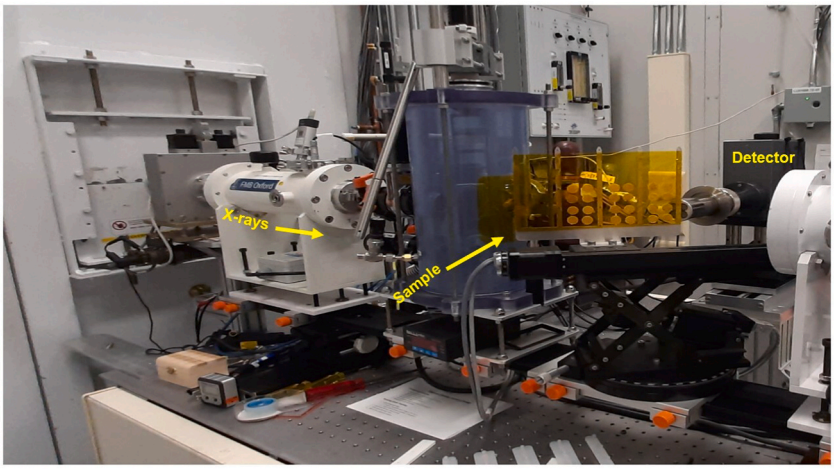

Fig. 1. The layout of the IDEAS-XRF beamline during data acquisition of Canadian Light Source, Saskatoon.

2.2. Storage experiment

Five-hundred-gram samples of each variety were conditioned to a moisture content (mc) of 17 % (wb) using distilled water in triplicates and then stored in airtight glass jars (volume 1 L) and these procedures were repeated every week for up to five week. Then, glass jars were stored at ambient conditions where storage temperatures were in the range of 22-25 °C. The mc was determined 24 h after conditioning by oven drying of 10 g samples at 130 °C for 19 h and the samples were reconditioned, if necessary, to maintain mc at 17 ± 0.5 % [37].

2.3. Bulk X-ray fluorescence spectroscopy

2.3.1. Sample preparation

Technical replicates were employed during the preparation of samples for bulk X-ray fluorescence (XRF) analyses. The samples were pulled from the three jars for grinding as a whole and three pellets were made as technical replicates. The purpose of using technical replicates was to ensure the reliability and reproducibility of the experimental results by accounting for any variability that might arise during the sample preparation process. The sample was first ground to fine powders using a cryo grinder (GENCO Spex 2010, Metuchen, NJ USA) using liquid nitrogen. Three circular pellets were prepared using a 13-mm diameter stainless steel die in a hydraulic press (PIKE Technologies, Madison, WI, USA) at three pressures (53.93, 34.32, and 14.70 kPa) with a holding of time 3 s for each pressure. The use of pressed pellets gives more accurate results compared to packed powder samples [38]. Ninety-seven milligrams of wheat flour were pressed into pellets of an approximate thickness of 0.2 mm and diameter of 13 mm (Fig. 1). The used die was wiped using ethanol after each sample and pellets were stored in the dark in a vacuum desiccator until further use [23].

2.3.2. Data acquisition and analysis

Data acquisition was carried out at the Industry Development Education Applications Students (IDEAS), which is a bending magnet beamline at the Canadian Light Source (CLS) (Fig. 1). Incident X-ray of energy of 13.6 keV was used in scanning of sample pellets and scanning was performed as per the procedure established [23]. The sample stage was placed between the source and detector at an angle of 45° and the detector distance from the sample was set to 11 mm. A beam size of 5 mm width and 2 mm height was used for sample scanning. Total of twenty-four sample pellets were mounted on the sample stage using Kapton tape. Three spectra were collected per pellet and each spectrum was completed in 85 s. Data acquisition was carried out using an in-house developed Aquaman software and then further data processing was done using PyMca (5.6.7) software [39]. The configuration and a calibration fit were developed using one representative sample spectrum and the rest of the sample analysis was completed using the batch fitting routine. The statistical analysis (one way ANOVA) was done to check significant differences in fluorescence count of nutrients (Fe, K, Zn, Ca and Mn) in the samples stored for 1 week, 3 week, 5 week, and control in MS-Excel 2008 and results are discussed in the discussion section.

2.4. X-ray fluorescence imaging

2.4.1. Sample preparation

Seeds were embedded in a Leica Cryogel using liquid nitrogen. The seeds were thin-sectioned to 80 μm thickness as per the described procedure [40] using a Leica CM1950 cryostat microtome (Leica Biosystems Inc., Richmond Hill, ON). Thin sections of samples reduce the distortion of the elemental maps caused by the penetrating nature of the X-rays [41]. Multiple sample sections on Kapton tape were placed on the sample holder of the BioXAS-Imaging beamline at the CLS (Fig. 2). The microscopic images were

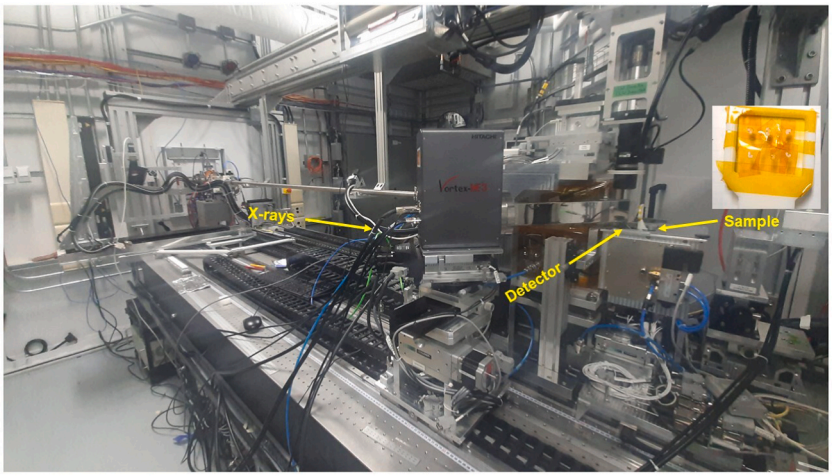

Fig. 2. BioXAS-imaging beamline and sample setup of Canadian Light Source, Saskatoon.

collected using digital microscope (Motic DM143, Motic, Kowloon, Hong Kong) before SR-XFI imaging of samples.

2.4.2. Data acquisition and analysis

The X-ray fluorescence imaging data were collected using the BioXAS-Imaging beamline at the CLS. The in-vacuum undulator of the beamline provides a high spectral brightness source for X-rays. In this study, the incident beam energy was set to 15 keV. The focused beam spot size was 5 μm × 5 μm. Data were collected in continuous bi-directional fly-scanning mode with a step size of 5 μm and 100 ms dwell time. Each seed section took about 8 h to scan. The Vortex-ME3 silicon drift X-ray detector (Hitachi High Technologies Science American, Inc. Chatsworth, CA) was at 45° and the samples were in a 90-degree stage configuration to the incident beam. The detector to the sample distance was set to 3.5 cm. Data acquisition was carried out using PyAcq data acquisition software. Calibration of elemental peaks and data fitting was carried out using PyMca (5.6.7) [39]. The batch fitting of data was carried out to generate the distribution of elements and further data were normalized using an RGB calculator of PyMca.

2.5. Mid infrared (mid-IR) spectroscopy

2.5.1. Sample preparation

Technical replicates were formed by selecting (pooling) wheat seeds from three jars and then grinding these to fine powders using a cryo grinder (GENCO Spex 2010, Metuchen, NJ USA) using liquid nitrogen. Fine flours (4.85 mg) were mixed with 385 mg potassium bromide (KBr) to make three powder pellets. Then, this mixture was ground again using the cryo grinder and then three equal portions of material were pressed using a hydraulic press (PIKE Technologies, Madison, WI, USA) at three pressures (53.93, 34.32, and 14.70 kPa) with holding time 3 s each time to form three pellets (13 mm in diameter) for each sample.

2.5.2. Data acquisition and analysis

Biochemical components (protein, lipid, and carbohydrates) were determined using mid infrared spectroscopy [34]. The pelleted sample was placed in a sample wheel for FTIR data collection. Data were collected using Cary 670 series microscope (Agilent Technologies Inc., Santa Clara, CA) equipped with a bulk analysis accessory and thermoelectrically cooled Deuterated Lanthanum α-Alanine doped TriGlycine Sulphate (DLaTGS) detector. The spectra were collected in the 4000-900 cm^{-1} range at 4 cm^{-1} resolution with 64 scans co-added at each raster point. Data processing and analysis were carried out using the Quasar software (version 1.5.0) [42] and OriginPro was used for plotting the spectra. The acquired spectra underwent several preprocessing steps to ensure data quality and reliability. These steps encompassed background correction, normalization based on sample concentration, baseline

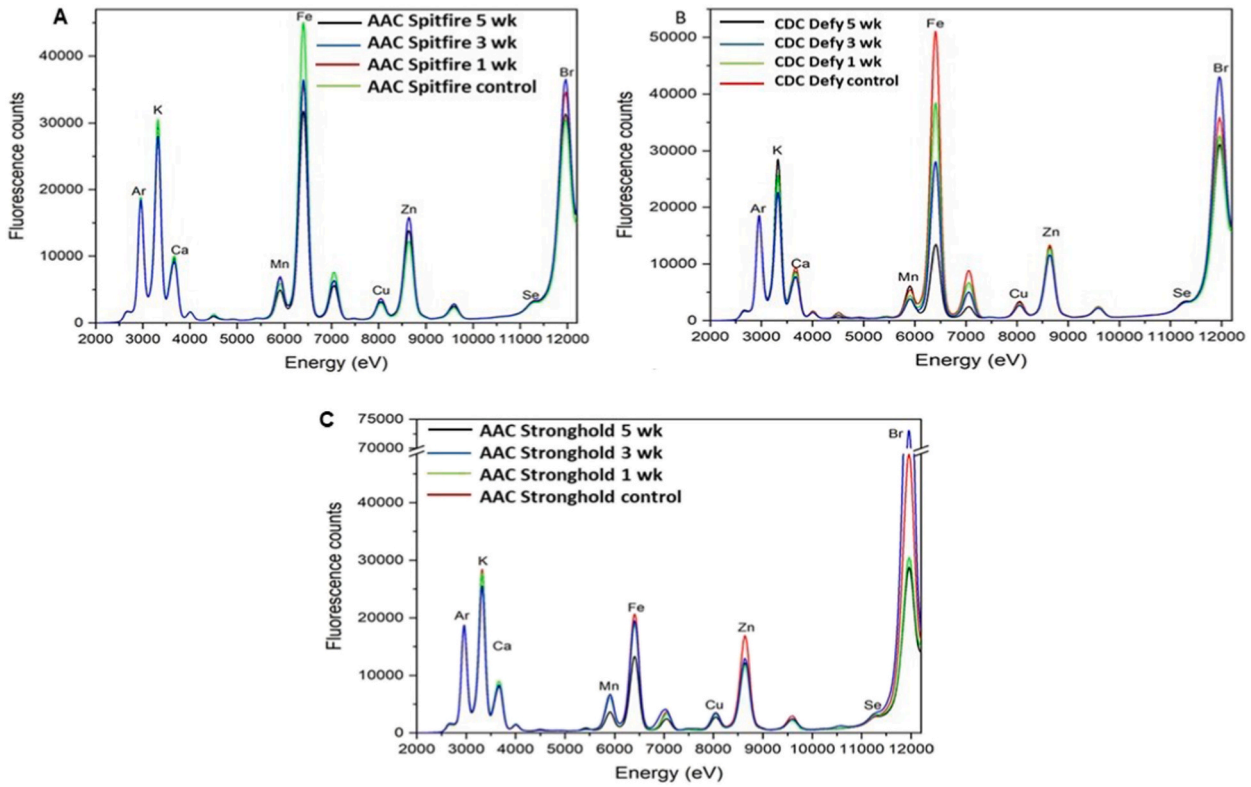

Fig. 3. XRF bulk spectra of durum wheat (A: AAC Spitfire, B: CDC Defy, and C: AAC Stronghold) in control (dry) and stored at different week at 17 % mc (wb).

correction utilizing the rubber band method, and vector normalization in Quasar software (Version 1.5.0). The reshaped combined dataset, comprising both healthy and damaged samples, underwent an application of principal component analysis (PCA) which is a well-established method for data reduction, wherein the dataset is transformed into a smaller number of components that encapsulate most of the original data's information. The initial and secondary principal components (PCs) were of particular interest in this analysis.

3. Result and discussion

The physical condition of three varieties stored for 5 week was assessed by visual observation of three replicates and found varying levels of deterioration compared to control samples. The fungus was visible on some of the germ parts of the AAC Spitfire and CDC Defy. Slight discoloration from yellow to faded yellow/blackish was also found on AAC Spitfire and CDC Defy. The AAC stronghold variety showed less deterioration on the surface or near the germ compared with other two varieties. The level of deterioration increased from the first week to fifth week in the selected varieties.

3.1. Micro and macro-nutrients presence

Bulk analysis of samples using spectroscopy of durum wheat varieties provided an overall picture of how much particular nutrient was present before and after storage and more insight into whether spoilage has any impact on their presence (Fig. 3). The higher photon counts were found for control samples than stored wheat samples for targeted nutrients. Nutrients Ca, K, Mn, Fe, Cu, Zn, and Br were located with peaks in durum samples at photon energies 3660 eV, 3320 eV, 5900 eV, 8000 eV, 8650 eV, and 12000 eV, respectively as shown in Fig. 3. The variation in nutrients Ca, K, Mn, Fe, Cu, Zn, and Br peaks was found among the three selected varieties. In control samples, the nutrient Fe was the highest in AAC Spitfire (Fig. 3A) followed by CDC Defy and the lowest in the AAC Stronghold. The stored samples of AAC Spitfire and CDC Defy showed differences in Fe peaks as compared to control. Maximum

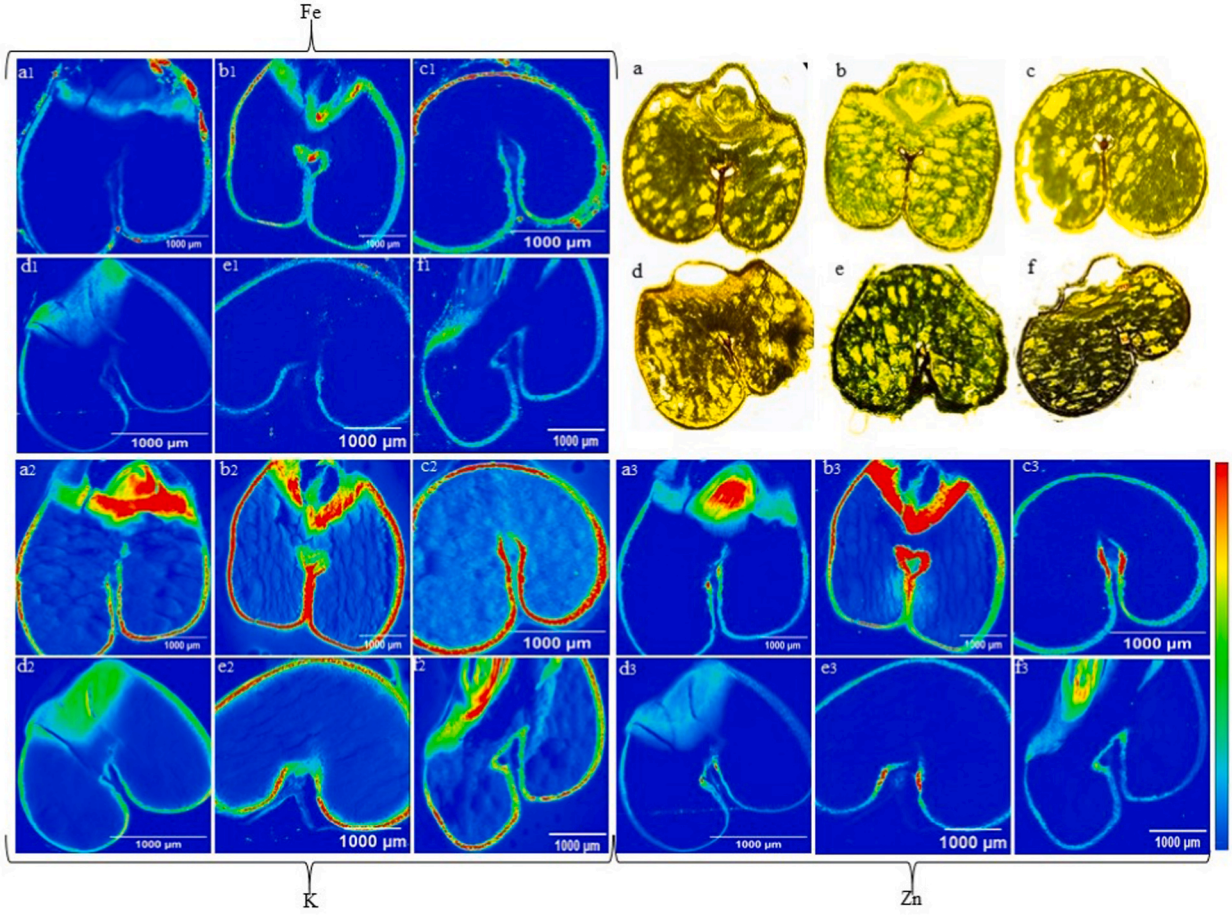

Fig. 4. The mapping of nutrients in control and 5 week stored durum wheat. Distribution of nutrients Fe (a1, b1, c1, d1, e1, f1), K (a2, b2, c2, d2, e2, f2) and Zn (a3, b3, c3, d3, e3, f3) using SR-XFI. Microscopic images of durum wheat control thin sections (a: AAC Spitfire, b: CDC Defy, c:AAC Stronghold) and 5 week stored (d: AAC Spitfire, e: CDC Defy, f: AAC Stronghold).

reduction of around 40 % in Fe fluorescence count was observed in 5 week stored samples over control samples. In case of AAC Stronghold, less variation about 20 % in Fe peaks was observed in 5 week stored samples over control. These results agreed with the visual inspection, where more spoilage was observed in AAC Spitfire and CDC Defy. The large variation of nutrient Fe was found in our results and it can be linked to fungal infection. One of the reasons for variation in nutrient Fe can be due to growth of fungus on durum wheat, as per literature fungal infection might strive on plant cells iron for support of their metabolic activities [43]. In fungi, intracellular siderophores can serve as iron storage [44]. One more reason for large variation of Fe element could be linked to deterioration of two durum wheat varieties (AAC Spitfire and CDC defy) where the outermost layer from whole grain was lost in sample preparation (may be damaged due to weak structure) where Fe is distributed. One of the study, stated that whole wheat contains Fe about 3.9 mg/100 g, as compared to wheat flour 0.9 mg/100 g [45], hence due to deterioration the Fe present in outer layers or attached husk, which may have fallen off at the end of 5 week of storage, could not make into wheat flour of pellets. In CDC Defy variety (Fig. 3B), the steep decline in Fe peak was observed as storage period progressed from 1 week to 5 week. A similar trend was observed in case of nutrient K and Zn in 5 week stored samples of durum wheat and reduction by 15 % in photon counts compared to control. The roles of micro-nutrients in plant defense were documented for Zn [20–22]. Hence from the seed defence point of view degradation of Zn and Mn micronutrients can be sign of deterioration in durum wheat.

In all durum varieties, minor degradation of nutrients (Ca, Mn, and Cu) was also observed due to deterioration. The around 8–10 % reduction in fluorescence counts was observed for Ca, Mn, and Cu nutrients in spoiled samples of durum wheat. As the storage time increased, it had an observable impact on K, Mn, and Fe, whereas Ca, Zn, and Cu had less variations. Durum wheat variety AAC Stronghold (Fig. 3C) showed a higher presence of nutrient Br and had variations among the samples stored for different week and remaining other nutrients were least affected or had less variation but showed comparatively higher variation in Zn. The nutrients Fe, Zn and Mn are essential for growth of fungus in cereals [46]. As discussed earlier in case of Fe presence that fungal or mould growth due to unfavorable condition during storage might be responsible for diminishing of nutrients. As per Bamrah et al. [23] the results obtained using the XRF spectroscopy method are statistically not different from the analytical laboratory methods for seed nutrient analysis, it means observed results in variation of nutrient due to deterioration can be used in further analysis or interpretation. In case of AAC Spitfire and CDC Defy, the decrease in counts or variation in peaks was observed from one-week storage onwards, whereas AAC Stronghold variety did not show reduction in counts until 3 week storage. These observations can be linked to deterioration of samples, where AAC Stronghold performed better in storage and three varieties can be characterised based on changes in macronutrients and micronutrients. All three varieties of durum wheat showed variable response in spectra of available nutrients; hence synchrotron X-ray fluorescence spectroscopy can be used in characterization of wheat varieties for post harvest storage. One-way ANOVA revealed statistically significant differences in means of fluorescence counts ($p < 0.05$) in some nutrients. In all selected varieties of durum wheat, the significant changes in ($p < 0.05$) nutrient Fe, Zn, and Mn were found during length of storage. The changes in nutrient K was found statistically insignificant ($p > 0.05$) in variety AAC Spitfire but was found significant in CDC Defy and AAC Stronghold ($p < 0.05$) varieties. The changes in nutrients Ca and Cu were found statistically insignificant at ($p > 0.05$) in all durum wheat varieties. The results illustrate that, deterioration of durum wheat had significant impact on its available nutrients at the end of 5 week storage.

3.2. *Changes in nutrient distribution*

The results of SR-XFI imaging of 80-μm thin sections of durum wheat (control and 5 week stored) are presented in Fig. 4. The purpose was to map changes in the distribution of essential nutrients within seed components before and after storage. Gradients in micronutrients and macronutrients were observed between spoiled and control durum wheat samples. The red in the scale represents maximum value and blue represents the minimum value of detected nutrient across wheat sections. In Fig. 4, only those sections in which maximum difference in nutrient distribution was observed are presented. Nutrient Fe was abundantly distributed in the seed coat (with aleurone layer) of the durum wheat in control samples in the order CDC Defy > AAC Spitfire > AAC Stronghold as is visible in Fig. 4 (a1, b1, c1) before storage and after storage in spoiled samples as in order CDC Defy > AAC Stronghold > AAC Spitfire Fig. 4 (d1, e1, f1). Next to Fe, the nutrient K was well distributed in all control samples of three varieties inside the seed coat and across the endosperm of the seed as shown in Fig. 4 (a2, b2, and c2). In spoiled samples nutrient K was found in the order CDC Defy > AAC Stronghold > AAC Spitfire as observed from Fig. 4 (d2, e2, f2). The distribution of K was also lowered in spoiled samples as observed from Fig. 4 (d2, e2 and f2). The observed distribution of K was lowered in endosperm, but not in the seed coat in durum wheat, this might be due to the deterioration of endosperm due to spoilage in the seed. Larger gradients were observed in Fe, Zn, and K in spoiled samples than controls.

Elements Cu, Fe, and Zn are localized in aleurone layer in wheat and large gradients in concentration of elements (Cu, Fe, Zn, Mn) exist between crease and endosperm region [24]. In this study only distribution of elements of interest were mapped not the concentration; however, in previous studies wheat seed components were characterized on the basis of element concentrations [24,47]. The distribution of Fe, Zn, and K was lowered in all spoiled samples as is visible in Fig. 4. Control samples of AAC Spitfire and CDC Defy showed Zn concentrated in germ and adjoined aleurone layer, but later in spoiled samples the distribution was lowered in all durum wheat samples Fig. 4 (a3-f3). In CDC Defy, Zn was found to be distributed in aleurone and crease region after 5 week Fig. 4 (b3); however, lower than control samples Fig. 4 (e3). An earlier study also reported that Zn is Associated with aleurone and crease regions [47]. Zinc plays a pivotal function in the plant's response to pests and diseases [48]. The major changes in Fe and K nutrient distribution were observed in scanned spoiled seed samples and these findings agreed with the findings of bulk XRF spectroscopy. As compared to K, Fe, and Zn, a minor variation in the distribution of other nutrients was observed for Ca, Mn, and Cu in the case of all durum varieties. The microscopic images of spoiled samples Fig. 4d, e, f showed deterioration in the endosperm over control samples Fig. 4a, b, c. The presence of air gaps and cracks were found in microscopic images of control samples in AAC Spitfire (Fig. 4a) and CDC

Defy (Fig. 4b). These imperfections may have been caused due to deterioration during storage or sample preparation, where major changes were observed in nutrients in spoiled sections as discussed earlier. The extent of damage was less in both thin sections of the AAC Stronghold as shown in Fig. 4c, f.

In our study, we were able to map variations in the distribution of micro-as well as macro-nutrients in durum wheat during post-harvest storage, because, in earlier studies, only effect of field treatments on the presence of nutrients in different cultivars was studied [19,24]. The nutrients Mn, Cu, Fe, and Zn play an important role in plant defense and immune responses [20–22]. Manganese is responsible for the production of phenolic compounds, which assist in plant defense mechanisms [49]. Almost similar trend was observed in decreasing distribution of nutrients in durum wheat cross sections for other nutrients Ca, Mn, and Cu, but gradients were lower than for Fe, Zn, and K. The variety AAC Stronghold performed better than other two varieties, but all durum wheat were affected at 17 % mc within 5 week of storage. The spoilage in storage not only affects physical structure, which was found in microscopic images, but also diminishes the nutritive value of durum wheat. The outcomes of nutrient mapping were found to be interconnected with the findings obtained from bulk spectroscopy analysis.

3.3. Biochemical changes

The changes in biochemical components during storage using mid-infrared spectroscopy analysis are presented in Figures (5-7). The variations in proteins, lipids, and carbohydrates in durum wheat varieties due to spoilage during storage were assessed and the spectra of control and 5 week stored wheat are presented in Fig. 5. The 1800–1100 cm^{-1} region of spectra was used in the analysis because this region is dominated by absorption bands related to protein, lipid, and carbohydrates [35]. Control samples of wheat have relatively higher lipids, proteins, and carbohydrates at 1740, 1650, and 1080 cm^{-1} [50]. The region 1200-900 cm^{-1} represent carbohydrates with peaks at 1023, 1080 and 1150 cm^{-1}, in which spectral bands located at 1080 and 1023 cm^{-1} have been attributed to starch and, the band observed at 1150 cm^{-1} can be attributed to the stretching of CC and CO bonds within starch molecules, as suggested by previous studies [34]. The control AAC Spitfire showed maximum absorbance for carbohydrates followed by CDC Defy and AAC Stronghold. Later, at the end of 5 week of storage large gradient was observed in absorbance of carbohydrates for AAC Spitfire compared to other two varieties CDC Defy and AAC Stronghold. The variety CDC Defy showed lower absorption for carbohydrates at the end of 5 week of storage, this illustrates impact of deterioration on biochemical composition and AAC stronghold showed less changes compared to other two varieties. Carbohydrates were degraded mostly may be due to starch degradation compared to lipids and proteins, which can be inferred from normalized spectra of CDC Defy and AAC Spitfire.

Durum wheat is called hard wheat due to its high protein content [13], hence it is important to know the impact of deterioration on wheat protein. Mid-IR may help in characterization of selected durum wheat on these changes due to deterioration in storage. Therefore, second derivatives of spectra were plotted for regions 1700-1600 cm^{-1} as shown in Fig. 6. The band regions at 1600–1500 cm^{-1} and 1700–1600 cm^{-1} represent the protein spectra with amide I at 1650 cm^{-1} (C═O and C–N stretching) and amide II at 1540 cm^{-1} (N–H bending and C–H stretching) [34]. The nature of proteins can be evaluated from Fig. 6. The peaks located at 1635 and 1654 cm^{-1} were β-sheets and α-helical secondary protein structures in durum wheat. All observed peaks followed similar pattern, but considerable variation was observed in 5 week stored samples for AAC Spitfire and CDC Defy varieties compared to control. It can be

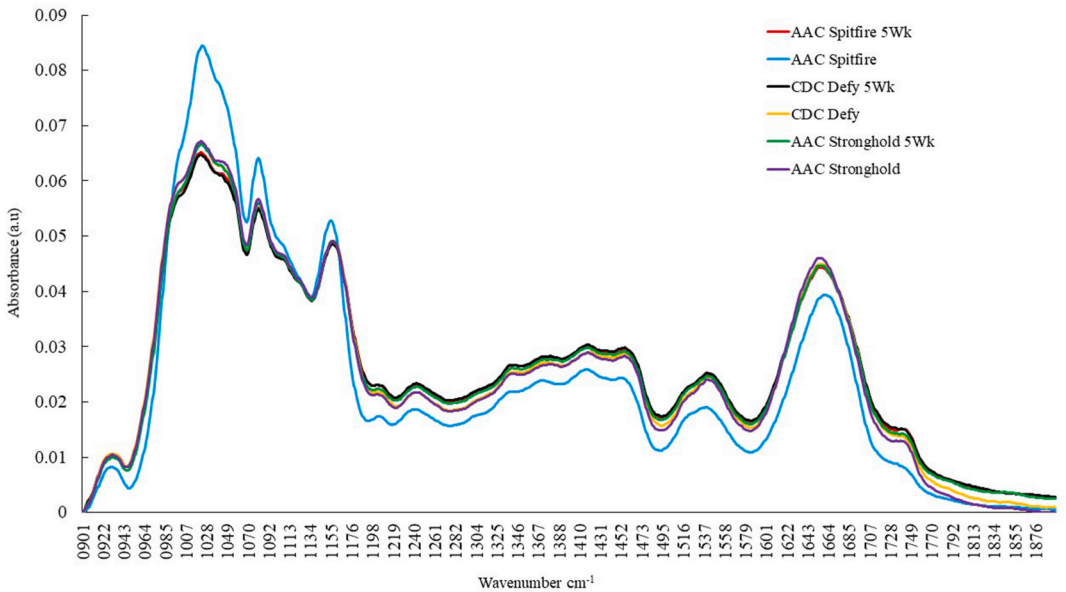

Fig. 5. Normalized bulk mid-IR spectra of durum wheat varieties; AAC Spitfire, CDC Defy and AAC Stronghold stored for 5 week and control to check biochemical (proteins, lipids, carbohydrates) variation in spectral region 1900-900 cm^{-1}..

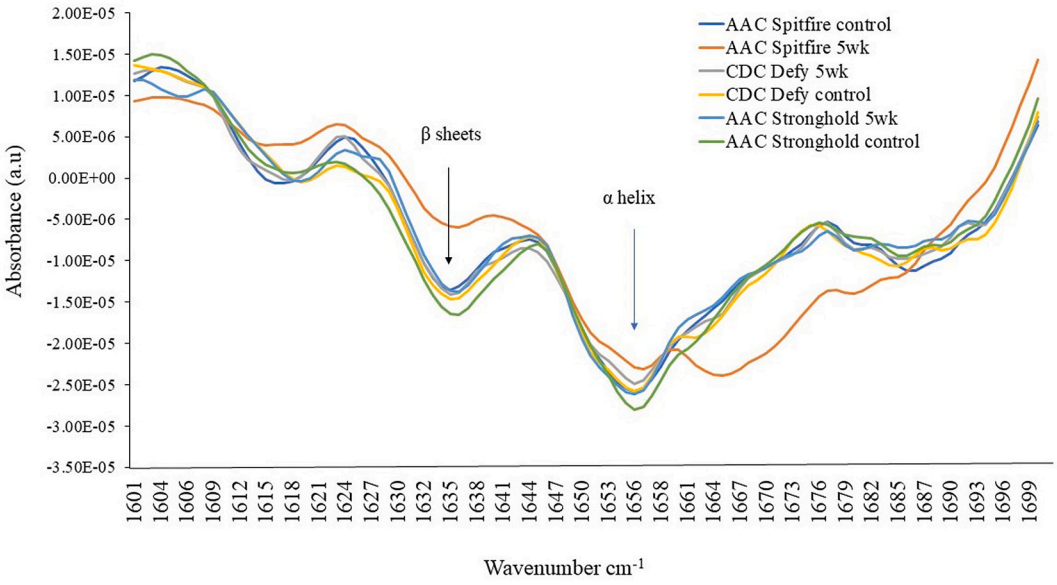

Fig. 6. The second derivative bulk mid-IR spectra of durum wheat varieties; AAC Spitfire, CDC Defy and AAC Stronghold stored for 5 week and control in spectral region 1700-1600 cm^{-1} for analysis of changes in protein and its structure.

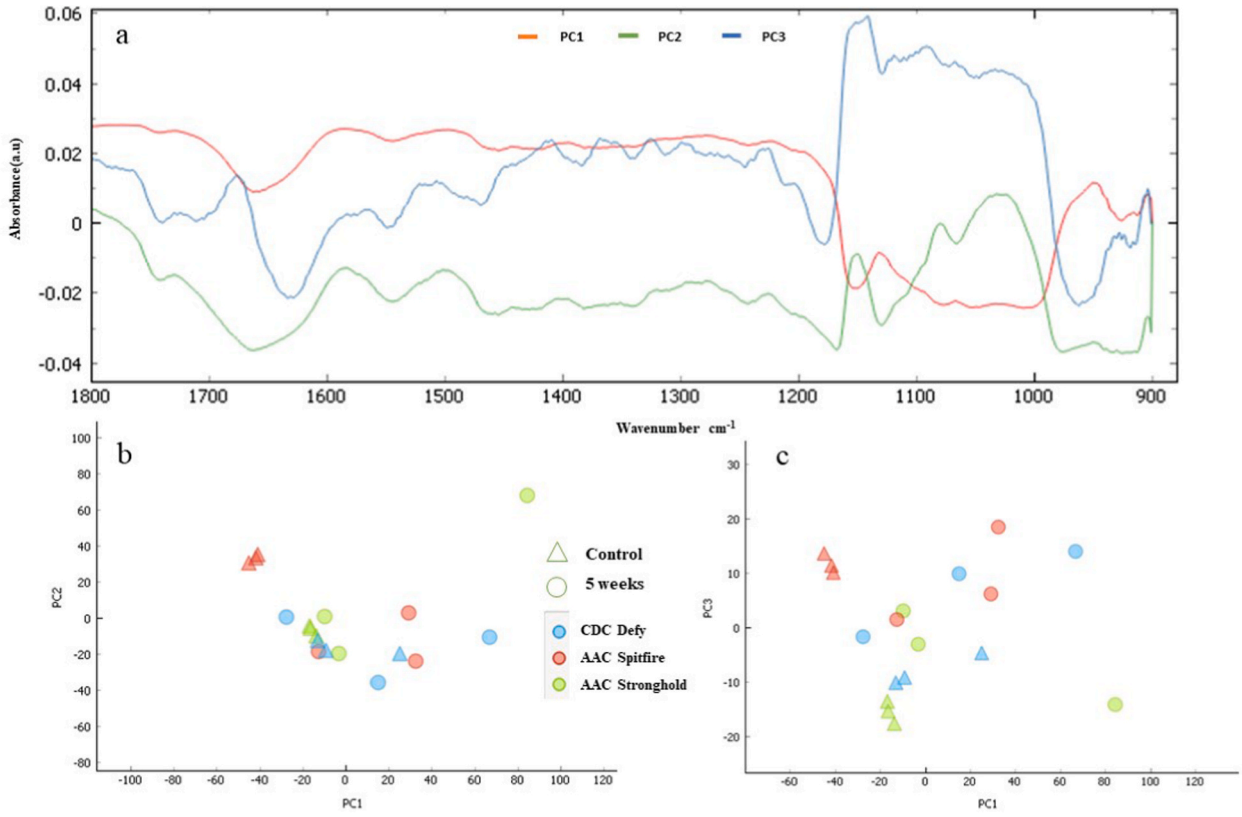

Fig. 7. Top (a): data loading plots of three principal components (PC1, PC2, PC3) of the data (durum wheat varieties; AAC Spitfire, CDC Defy and AAC Stronghold stored for 5 week and control) in spectral region 1800-900 cm^{-1}. Bottom: Principal component analysis (b) (PC1 vs PC2) of durum wheat. Principal component analysis (c) (PC1 vs PC3) of durum wheat varieties.

observed protein (1700–1500 cm^{-1}) regions play an important role in the characterization of durum wheat. AAC Spitfire control and 5 week stored wheat showed variation in lipid peaks at 1750 cm^{-1} as presented in the second derivative spectra of Fig. 6. Biochemical changes in storage studies wheat and other cereals at unsafe moisture were summarized [51] and found that protein, carbohydrates were decreased in range of 3–19 % after 6 week storage due to mould growth. Lipids were at 77 % of original value in wheat and processed wheat products after end of storage due to fungal infection [51]. The analysis of principal components revealed that the first three principal components (PCs) PC1, PC2 and PC3 collectively showed 73 %, 20 % and 5 % of the explained variance, respectively (Fig. 7a). By employing the PC scores, a clear distinction was observed between the PC scores generated for control samples and 5 week stored samples. These PC scores were further utilized to create a graphical representation Fig. 7b, c. The score of 5 week stored samples are bent to right side than that of control samples which were clustered at left side. In the resulting plot a discernible separation between the PC scores corresponding to control and 5 week stored wheat was evident. The deterioration in seed tends to be non-uniform, hence not all tissues of seed would necessarily experience damage, therefore, some 5 week stored samples showed up in left side with controls in the plot. In summery, more affected varieties due to spoilage were AAC Spitfire and CDC Defy and less affected was the AAC Stronghold. The control sample of AAC Spitfire was in the negative region than the other two varieties, which might reflect its initial condition that it has poor storability. Similar result was reported for fusarium susceptible and resistant wheat varieties [33], where they were able to characterize fusarium resistant varieties of wheat based on FTIR spectra results. The plot revealed that almost all durum wheat showed deterioration as per shifting of scores in negative region. AAC Stronghold was sound before storage but later showed deterioration, but less compared to other two varieties. The kernel texture and biochemical composition, including starch granule texture, and protein content vary among wheat varieties [52] and similar findings were the outcome of this study. In deterioration process, fungi can absorb and metabolize a diverse range of soluble carbohydrates, insoluble ones like starches, cellulose, and hemicelluloses and break down complex hydrocarbons such as lignin [53]. The durum wheat is said to be poor in storage under unfavorable conditions [4] and in our study using high resolution imaging it was found more susceptible to spoilage in short term storage.

4. Conclusion

The SR-XRF analysis revealed the effect of storage time and deterioration on variations in micro and macro nutrients. The SR-XFI imaging revealed changes in nutritional distributions at the micron scale in thin sections in their maps within seed features. The changes in biochemical components (proteins, lipids, and carbohydrates) due to deterioration during storage were determined using mid-infrared (mid-IR) spectroscopy. The AAC Spitfire and CDC Defy varieties showed more deterioration than AAC Stronghold, and all three varieties can be characterized based on variation in nutrient and their distribution with spoilage and storage time. The developed methodology in this study will be useful in the analysis of more cereal and pulse seeds. There is good scope of linking observed changes in wheat during storage to X-ray microcomputed tomography data (microstructural data) of wheat.

Data availability statement

Data will be made available on request.

CRediT authorship contribution statement

Navnath S. Indore: Methodology, Project administration, Writing – review & editing. **Chithra Karunakaran:** Data curation. **Digvir S. Jayas:** Conceptualization, Funding acquisition, Supervision, Writing – review & editing. **Viorica F. Bondici:** Investigation, Resources. **Miranda Vu:** Investigation, Resources. **Kaiyang Tu:** Investigation, Resources. **David Muir:** Investigation, Resources.

Declaration of competing interest

None of the co-authors have any conflict of interest to declare for the paper entitled “Mapping biochemical and nutritional changes in durum wheat due to spoilage during storage authored by Indore Navnath S., Chithra Karunakaran, Digvir S. Jayas, Viorica F Bondici, Miranda Vu, Kaiyang Tu and, David Muir”.

Acknowledgement

The authors acknowledge the Netaji Subhash Chandra fellowship from the Indian Council of Agricultural Research (ICAR), India via grant no. ICAR/2019 for the first author and the Natural Sciences and Engineering Research Council of Canada for supporting the student research via a grant no. RGPIN-2018-04420 to Dr Jayas. The authors also acknowledge the Canadian Light Source, Saskatoon for providing beamtime and access to conduct experiments.

References

[1] B.L. Beres, E. Rahmani, J.M. Clarke, P. Grassini, C.J. Pozniak, C.M. Geddes, K.D. Porker, W.E. May, J.K. Ransom, A Systematic review of durum wheat: enhancing production systems by exploring genotype, environment, and management (G × E × M) Synergies, Front. Plant Sci. 11 (2020) 1–14, https://doi.org/10.3389/fpls.2020.568657.

[2] LMC International, The Economic Impact of Canola on the Canadian Economy: 2020 Update Insights for Agribusiness Specialist Data and Analysis for Commercial Decision-Making, 2020. https://cerealscanada.ca/wheat/.
[3] Statistics Canada, Model-based Principal Field Crop Estimates, 2022. https://www150.statcan.gc.ca/n1/daily-quotidien/220914/dq220914b-eng.htm.
[4] U. Nithya, V. Chelladurai, D.S. Jayas, N.D.G. White, Safe storage guidelines for durum wheat, J. Stored Prod. Res. 47 (2011) 328–333, https://doi.org/10.1016/j.jspr.2011.05.005.
[5] D.S. Jayas, Storing grains for food Security and Sustainability, Agric. Res. 1 (2012) 21–24, https://doi.org/10.1007/s40003-011-0004-4.
[6] H.A.H. Wallace, P.L. Sholberg, R.N. Sinha, W.E. Muir, Biological, physical and chemical changes in stored wheat, Mycopathologia 82 (1983) 65–76, https://doi.org/10.1007/BF00437333.
[7] E. Schroth, W.E. Muir, D.S. Jayas, N.D.G. White, D. Abramson, Storage limit of wheat at 17% moisture content, Can. Agric. Eng. 40 (1998) 201–205.
[8] M. Schmidt, S. Horstmann, L. De Colli, M. Danaher, K. Speer, E. Zannini, E.K. Arendt, Impact of fungal contamination of wheat on grain quality criteria, J. Cereal. Sci. 69 (2016) 95–103, https://doi.org/10.1016/j.jcs.2016.02.010.
[9] S.-B. Zhang, Y.-Y. Lv, Y.-L. Wang, F. Jia, J.-S. Wang, Y.-S. Hu, Physiochemical changes in wheat of different hardnesses during storage, J. Stored Prod. Res. 72 (2017) 161–165, https://doi.org/10.1016/j.jspr.2017.05.002.
[10] Q.-S. Yuan, P. Yang, A.-B. Wu, D.-Y. Zuo, W.-J. He, M.-W. Guo, T. Huang, H.-P. Li, Y.-C. Liao, Variation in the microbiome, trichothecenes, and aflatoxins in stored wheat grains in wuhan, China, Toxins 10 (2018) 171, https://doi.org/10.3390/toxins10050171.
[11] A.F. Worku, K.K. Kalsa, M. Abera, H.G. Nigus, Effects of storage strategies on physicochemical properties of stored wheat in Ethiopia, AIMS Agric. Food. 4 (2019) 578–591, https://doi.org/10.3934/agrfood.2019.3.578.
[12] C. Karunakaran, R. Lahlali, N. Zhu, A.M. Webb, M. Schmidt, K. Fransishyn, G. Belev, T. Wysokinski, J. Olson, D.M.L. Cooper, E. Hallin, Factors influencing real time internal structural visualization and dynamic process monitoring in plants using synchrotron-based phase contrast X-ray imaging, Sci. Rep. 5 (2015), 12119, https://doi.org/10.1038/srep12119.
[13] S. Neethirajan, C. Karunakaran, S. Symons, D.S. Jayas, Classification of vitreousness in durum wheat using soft X-rays and transmitted light images, Comput. Electron. Agric. 53 (2006) 71–78, https://doi.org/10.1016/j.compag.2006.03.001.
[14] S. Neethirajan, D.S. Jayas, N.D.G. White, H. Zhang, Investigation of 3D geometry of bulk wheat and pea pores using X-ray computed tomography images, Comput. Electron. Agric. 63 (2008) 104–111, https://doi.org/10.1016/j.compag.2008.01.019.
[15] A. Hughes, K. Askew, C.P. Scotson, K. Williams, C. Sauze, F. Corke, J.H. Doonan, C. Nibau, Non-destructive, high-content analysis of wheat grain traits using X-ray micro computed tomography, Plant Methods 13 (2017) 76, https://doi.org/10.1186/s13007-017-0229-8.
[16] T.D.Q. Le, C. Alvarado, C. Girousse, D. Legland, A.-L. Chateigner-Boutin, Use of X-ray micro computed tomography imaging to analyze the morphology of wheat grain through its development, Plant Methods 15 (2019) 84, https://doi.org/10.1186/s13007-019-0468-y.
[17] V. Radchuk, D. Weier, R. Radchuk, W. Weschke, H. Weber, Development of maternal seed tissue in barley is mediated by regulated cell expansion and cell disintegration and coordinated with endosperm growth, J. Exp. Bot. 62 (2011) 1217–1227, https://doi.org/10.1093/jxb/erq348.
[18] Y. Lv, P. Tian, S. Zhang, J. Wang, Y. Hu, Dynamic proteomic changes in soft wheat seeds during accelerated ageing, PeerJ 6 (2018), e5874, https://doi.org/10.7717/peerj.5874.
[19] M. Ciudad-Mulero, M.C. Matallana-González, M.J. Callejo, J.M. Carrillo, P. Morales, V. Fernández-Ruiz, Durum and bread wheat flours. Preliminary mineral characterization and its potential health claims, Agronomy 11 (2021) 108, https://doi.org/10.3390/agronomy11010108.
[20] C. Dordas, Role of nutrients in controlling plant diseases in sustainable agriculture. A review, Agron. Sustain. Dev. 28 (2008) 33–46, https://doi.org/10.1051/agro:2007051.
[21] H. Fones, G.M. Preston, The impact of transition metals on bacterial plant disease, FEMS Microbiol. Rev. 37 (2013) 495–519, https://doi.org/10.1111/1574-6976.12004.
[22] R. Graham, M. Webb, Micronutrients and disease resistance and tolerance in plants, in: Micronutr. Agric., 2018, pp. 329–370, https://doi.org/10.2136/sssabookser4.2ed.c10.
[23] R.K. Bamrah, P. Vijayan, C. Karunakaran, D. Muir, E. Hallin, J. Stobbs, B. Goetz, M. Nickerson, K. Tanino, T.D. Warkentin, Evaluation of X-ray fluorescence spectroscopy as a tool for nutrient analysis of pea seeds, Crop Sci. 59 (2019) 2689–2700, https://doi.org/10.2135/cropsci2019.01.0004.
[24] N. De Brier, S.V. Gomand, E. Donner, D. Paterson, E. Smolders, J.A. Delcour, E. Lombi, Element distribution and iron speciation in mature wheat grains (Triticum aestivum L.) using synchrotron X-ray fluorescence microscopy mapping and X-ray absorption near-edge structure (XANES) imaging, Plant Cell Environ. 39 (2016) 1835–1847, https://doi.org/10.1111/pce.12749.
[25] K. Tanaka, T. Yoshida, Z. Kasai, Distribution of mineral elements in the outer layer of rice and wheat grains, using electron microprobe x-ray analysis, Soil Sci. Plant Nutr. 20 (1974) 87–91, https://doi.org/10.1080/00380768.1974.10433231.
[26] S.P. Singh, K. Vogel-Mikuš, I. Arčon, P. Vavpetič, L. Jeromel, P. Pelicon, J. Kumar, R. Tuli, Pattern of iron distribution in maternal and filial tissues in wheat grains with contrasting levels of iron, J. Exp. Bot. 64 (2013) 3249–3260, https://doi.org/10.1093/jxb/ert160.
[27] S.P. Singh, K. Vogel-Mikuš, P. Vavpetič, L. Jeromel, P. Pelicon, J. Kumar, R. Tuli, Spatial X-ray fluorescence micro-imaging of minerals in grain tissues of wheat and related genotypes, Planta 240 (2014) 277–289, https://doi.org/10.1007/s00425-014-2084-4.
[28] M. Javid Iqbal, N. Shams, K. Fatima, Nutritional quality of wheat, in: Wheat, IntechOpen, 2022, https://doi.org/10.5772/intechopen.104659.
[29] G. Boggini, H. Namoune, J. Abecassis, B. Cuq, Other traditional durum-derived products, in: Durum Wheat, Elsevier, 2012, https://doi.org/10.1016/B978-1-891127-65-6.50015-5 or. 177–199.
[30] Cereals Canada, Crop Summary Grown in 2022, 2022. https://cerealscanada.ca/wp-content/uploads/2022/11/2022-New_Crop_Summary_FINAL_1122.pdf.
[31] D. Boyacioğlu, N.S. Hettiarachchy, Changes in some biochemical components of wheat grain that was infected with Fusarium graminearum, J. Cereal. Sci. 21 (1995) 57–62, https://doi.org/10.1016/S0733-5210(95)80008-5.
[32] A. Sharma, S. Garg, I. Sheikh, P. Vyas, H.S. Dhaliwal, Effect of wheat grain protein composition on end-use quality, J. Food Sci. Technol. 57 (2020) 2771–2785, https://doi.org/10.1007/s13197-019-04222-6.
[33] R. Lahlali, T. Song, M. Chu, C. Karunakaran, F. Yu, Y. Wei, G. Peng, Synchrotron-based spectroscopy and imaging reveal changes in the cell-wall composition of barley leaves in defence responses to Blumeria graminis f. sp. tritici, Can. J. Plant Pathol. 41 (2019) 457–467, https://doi.org/10.1080/07060661.2019.1581662.
[34] C. Karunakaran, P. Vijayan, J. Stobbs, R.K. Bamrah, G. Arganosa, T.D. Warkentin, High throughput nutritional profiling of pea seeds using Fourier transform mid-infrared spectroscopy, Food Chem. 309 (2020), 125585, https://doi.org/10.1016/j.foodchem.2019.125585.
[35] C.B. Singh, D.S. Jayas, F. Borondics, N.D.G. White, Synchrotron based infrared imaging study of compositional changes in stored wheat due to infection with Aspergillus glaucus, J. Stored Prod. Res. 47 (2011) 372–377, https://doi.org/10.1016/j.jspr.2011.07.001.
[36] P. Yu, D.A. Christensen, C.R. Christensen, M.D. Drew, B.G. Rossnagel, J.J. McKinnon, Use of synchrotron FTIR microspectroscopy to identify chemical differences in barley endosperm tissue in relation to rumen degradation characteristics, Can. J. Anim. Sci. 84 (2004) 523–527, https://doi.org/10.4141/A03-102.
[37] S. Joseph, Moisture Measurement — Unground Grain and Seeds, ASABE Stand. ASAE S352, 2017. http://refhub.elsevier.com/S0022-474X(22)00131-X/sref1.
[38] J.S. Watson, Fast, Simple method of powder pellet preparation for X-ray fluorescence analysis, X Ray Spectrom. 25 (1996) 173–174, https://doi.org/10.1002/(SICI)1097-4539, 199607)25:4<173::AID-XRS158>3.0.CO;2-Z.
[39] V.A. Solé, E. Papillon, M. Cotte, P. Walter, J. Susini, A multiplatform code for the analysis of energy-dispersive X-ray fluorescence spectra, Spectrochim. Acta Part B At. Spectrosc. 62 (2007) 63–68, https://doi.org/10.1016/j.sab.2006.12.002.
[40] E. Lombi, K.G. Scheckel, J. Pallon, A.M. Carey, Y.G. Zhu, A.A. Meharg, Speciation and distribution of arsenic and localization of nutrients in rice grains, New Phytol. 184 (2009) 193–201, https://doi.org/10.1111/j.1469-8137.2009.02912.x.
[41] E. Lombi, K.G. Scheckel, I.M. Kempson, In situ analysis of metal(loid)s in plants: State of the art and artefacts, Environ. Exp. Bot. 72 (2011) 3–17, https://doi.org/10.1016/j.envexpbot.2010.04.005.

[42] J. Demšar, T. Curk, A. Erjavec, Č. Gorup, T. Hočevar, M. Milutinovič, M. Možina, M. Polajnar, M. Toplak, A. Starič, M. Štajdohar, L. Umek, L. Žagar, J. Žbontar, M. Žitnik, B. Zupan, Orange: data mining toolbox in python, J. Mach. Learn. Res. 14 (2013) 2349–2353.
[43] J. Schindelin, I. Arganda-Carreras, E. Frise, V. Kaynig, M. Longair, T. Pietzsch, S. Preibisch, C. Rueden, S. Saalfeld, B. Schmid, J.Y. Tinevez, D.J. White, V. Hartenstein, K. Eliceiri, P. Tomancak, A. Cardona, Fiji: an open-source platform for biological-image analysis, Nat. Methods 9 (2012), https://doi.org/10.1038/nmeth.2019.
[44] U. Neubauer, B. Nowack, G. Furrer, R. Schulin, Heavy metal sorption on clay minerals affected by the siderophore desferrioxamine B, Environ. Sci. Technol. 34 (2000), https://doi.org/10.1021/es990495w.
[45] B. McKevith, Nutritional aspects of cereals, Nutr. Bull. 29 (2004), https://doi.org/10.1111/j.1467-3010.2004.00418.x.
[46] G.S. Rawla, A note on trace elements for the growth of nigrospora oryzae (b. And br.) Petch, New Phytol. 68 (1969) 941–943, https://doi.org/10.1111/j.1469-8137.1969.tb06493.x.
[47] T. Zhang, H. Sun, Z. Lv, L. Cui, H. Mao, P.M. Kopittke, Using synchrotron-based approaches to examine the foliar application of ZnSO 4 and ZnO nanoparticles for field-grown winter wheat, J. Agric. Food Chem. 66 (2018) 2572–2579, https://doi.org/10.1021/acs.jafc.7b04153.
[48] S.K. Gupta, A.K. Rai, S.S. Kanwar, T.R. Sharma, Comparative analysis of zinc finger proteins involved in plant disease resistance, PLoS One 7 (2012), e42578, https://doi.org/10.1371/journal.pone.0042578.
[49] F. Mendoza, P. Verboven, H.K. Mebatsion, G. Kerckhofs, M. Wevers, B. Nicolaï, Three-dimensional pore space quantification of apple tissue using X-ray computed microtomography, Planta 226 (2007) 559–570, https://doi.org/10.1007/s00425-007-0504-4.
[50] R. Saxton, O.M. McDougal, Whey protein powder analysis by mid-infrared spectroscopy, Foods 10 (2021) 1033, https://doi.org/10.3390/foods10051033.
[51] K.A. Rosentrater, Biochemical, functional, and nutritive changes during storage, in: Storage Cereal Grains Their Prod, 2022, https://doi.org/10.1016/B978-0-12-812758-2.00010-6.
[52] I. Pasha, F.M. Anjum, C.F. Morris, Grain hardness: a major determinant of wheat quality, Food Sci. Technol. Int. 16 (2010) 511–522, https://doi.org/10.1177/1082013210379691.
[53] David moore, Brittanica Nutrition, 1–5, https://www.britannica.com/science/fungus/Form-and-function-of-fungi, 2022. eskuratua 2023(e)ko abuztuakaren 29a.